

## Effect of high early strength cement and accelerator concentrations on the low-temperature compressive strength of concrete

Hyeong-Cheol Kim<sup>a,b</sup>, Tae-Beom Min<sup>b</sup>, Young-Bum Mun<sup>b</sup>, Jae-Young Kim<sup>b</sup>, Hyun-Kuk Choi<sup>b</sup> and Han-seung Lee<sup>a,\*</sup>

<sup>a</sup>Department of Architecture, Hanyang University, Ansan, Gyeonggi-do, Korea

<sup>b</sup>R & D Center, Sungshin Cement, Bugang-Myun, Sejong Special Self-Governing City, Korea

An important issue associated with wintertime construction is the ability to mix fresh concrete without it freezing. To obtain the required compressive strength, warm curing or heat curing is often performed at the construction site. However, both these methods are difficult to manage, incur the risk of fire, and have low energy efficiency, with excessive heat loss to the surrounding environment. To overcome these problems, here we evaluate the performance of concrete as a function of the concentrations of high early strength cement and accelerator for protection against freezing. Our aim is to develop a concrete with a compressive strength of 5 MPa within one day of aging to prevent early frost damage. We achieve this compressive strength development when the amounts of high early strength cement and accelerator exceed 15%. Increasing the amount of accelerator increases the early compressive strength by shortening the setting time and enhancing Ca(OH)<sub>2</sub> formation. Thus, early frost damage could be prevented in low-temperature concrete construction work without warm curing or heat curing when the water-to-binder ratio is reduced. The use of high early strength cement and an accelerator for freeze protection is optimized.

**Key words:** Freeze protection, Frost damage, High early strength cement, Accelerator, Winter concreting.

### Introduction

A major challenge for construction work during the winter is the preparation of fresh concrete that achieves the required compressive strength without freezing [1-3]. When the outdoor temperature drops below 0°C, partially cured concrete can be destroyed by early frost damage [4-6]. To prevent this, a minimum compressive strength of 5 MPa is required during early aging [7-9]. To reach this value, curing sheets or a curing roof can be installed after the concrete is poured at the construction site and the concrete can be warmed using lignite or a heater [10-11]. However, these heating methods can be difficult to manage and they include the risk of fire. In addition, heating is inefficient, with excessive heat loss to the environment surrounding the concrete [12-13]. Furthermore, the heating and hence the strength development is non-uniform, as it varies with the distance from the heat source, resulting in poor quality control [14]. Another heating method involves embedding a heating cable inside the concrete. A uniform concrete quality can be achieved using this method because it maintains a constant temperature. However, it is impossible to reuse the cable, as it remains embedded in the concrete [15]. The heat supply would be interrupted by coating disbondment cutting during

the pouring of the concrete. Thus, the heating cable method can be applied only in special cases [15-17].

In an attempt to overcome such problems, in this study, we optimized the concentrations of high early strength cement and an accelerator in concrete with the aim of achieving a compressive strength of 5 MPa within one day of aging. Accordingly, the compressive strength of the concrete was evaluated as a function of the concentrations of the high early strength cement and accelerator. The hydration products, produced during the hydration reaction between the high early strength cement and the accelerator at temperatures below 0 °C, were characterized by microanalysis methods. In addition, the characteristics of the hydration reaction at low temperature were investigated. Such analyses could provide valuable information for the construction industry, in particular by providing an alternative to the heat curing of concrete in cold conditions.

### Accelerators for Freeze Protection

#### Inorganic accelerators

Existing inorganic accelerators for freeze protection include calcium chloride, fluorine, silicate, aluminate, thiosulfate, and calcium formate. The molecular structures of three inorganic accelerators are shown in Fig. 1. Calcium formate promotes hydration by inhibiting the formation of the (CHOO-)C<sub>3</sub>S protective layer on the surface of concrete. When the inorganic accelerator is added to the cement, the hydration of C<sub>3</sub>S is accelerated, resulting in the maximum supersaturation of

\*Corresponding author:  
Tel : +82-31-400-5181  
Fax: +82-31-436-8169  
E-mail: ercleehs@hanyang.ac.kr

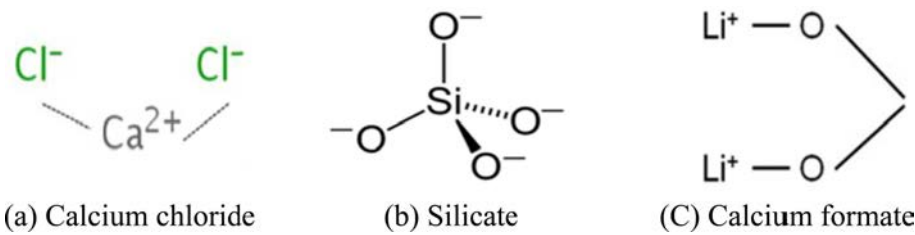


Fig. 1. Molecular structures of inorganic accelerators.

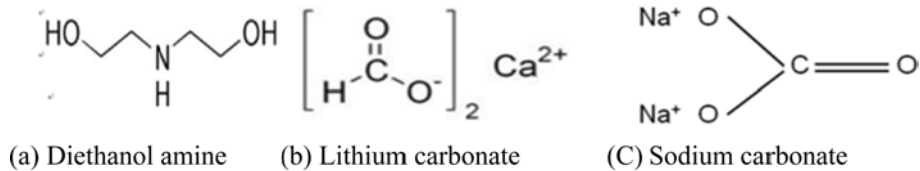


Fig. 2. Molecular structures of organic accelerators.

Ca(OH)<sub>2</sub> in solution. Meanwhile, the early compressive strength increases with the rapid precipitation of hydration products such as C-S-H gel. The compressive strength is increased with this precipitation, since the fibriform crystals create a fine microstructure of hydration products that increases the crystallization of the C-S-H gel.

### Organic accelerators

Existing organic accelerators for freeze protection include amine, nitrous acid, acrylic acid, lithium carbonate, sodium carbonate, and sodium gluconate. The molecular structures of some organic accelerators are shown in Fig. 2. For amine-based accelerators, ettringite is formed by the accelerators' reactions with gypsum. This accelerates the hydration reaction by accelerating the production of the monosulfate phase in ettringite.

## Experimental

In this study, we aimed to develop a concrete with a compressive strength of 5 MPa in one day of aging at -5 °C, using high early strength cement and an accelerator for freeze protection. We evaluated the compressive strength development and the performance of the concrete regarding the prevention of early frost damage. Moreover, we characterized the hydration products from the low-temperature reactions between the high early strength cement and the accelerator by microanalysis methods, including scanning electron microscopy (SEM), X-ray diffraction (XRD), and thermogravimetry/differential thermal analysis (TG/DTA). When fine aggregates were used in the samples during the microanalysis experiments, the reliability of the hydration product analysis was reduced because of the fine aggregate components. Hence, the microanalysis experiments were conducted only on cement pastes, which did not contain fine aggregates.

### Experimental design

Table 1 shows the different mortar and cement paste mixtures used for the various experimental

characterizations. A concrete mixture with a water-to-binder ratio (W/C) of 35% was selected to maximize the performance of the accelerator. The concentration of the accelerator was set to four times that of the added water. The experiments separately measured the concretes and the cement pastes. The specimens were air dry-cured at -5 °C. The fluid level in the concrete was measured according to ASTM C1611, while setting time tests were performed based on ASTM C191. In addition, compressive strength measurements were conducted based on ASTM C39. The microanalysis experiments were performed using five specimens from each of the cement pastes. The experimental samples and test conditions are shown in Table 2.

### Materials

In this study, ordinary Portland cement (OPC) and high early strength cement (HC) were used, with physical and chemical properties shown in Tables 3 and 4, respectively. The physical properties of the superplasticizer are shown in Table 5. Moreover, a

Table 1. Mix proportions of mortars and cement pastes.

Specimen	W/C	C	HC	W	S	G	AF	SP
	(%)	(kg/m <sup>3</sup> )			%			
OPC-0-C (plain)	35	471		165	745	943	-	0.85
3J-0-C	35		471	165	745	943	-	0.85
3J-10-C	35		471	148.5	745	943	16.5	0.85
3J-15-C	35		471	140.25	745	943	24.75	0.85
3J-20-C	35		471	132	745	943	33.0	0.85
OPC-0-P	35	1498	-	524	-	-	-	1
3J-0-P	35	-	1498	524	-	-	-	1
3J-10-P	35	-	1498	471.6	-	-	52.4	1
3J-15-P	35	-	1498	445.4	-	-	78.6	1
3J-20-P	35	-	1498	419.2	-	-	104.8	1

\*C: Cement; HC: High early strength cement; W: Water, S: Sand; AF: Accelerator for freeze protection; SP: Superplasticizer.

**Table 2.** Experimental samples and test conditions.

Experimental factors		Experimental levels	
W/C(%)		35	
Concentration of accelerator (%)		0, 10, 15, 20	
Measurement Items			
	Items	Standard	Age (days)
Concrete	Slump flow	ASTM C1611	–
	Setting time	ASTM C191	–
	Compressive strength	ASTM C39	1, 3, 7, 28
Conduction calorimetry (Measurement of hydration heat)		–	–
Cement paste	Measurement of Ca(OH) <sub>2</sub> generation (TG/DTA)	–	–
	Scanning Electron Microscope (SEM)	–	1, 3, 7, 28
	Hydrates by XRD analysis	–	1, 3

**Table 3.** Physical properties of ordinary Portland cement (OPC) and high early strength cement (HC).

Materials	Median particle size, d <sub>50</sub> (μm)	Blaine fineness (cm <sup>2</sup> /g)
OPC	18.85	3578
HC	8.14	4,457

**Table 4.** Chemical properties of ordinary Portland cement (OPC) and high early strength cement (HC).

Chemical composition	Ordinary Portland cement (%)	High early strength cement (%)
Silicon dioxide (SiO <sub>2</sub> )	21.86	21.16
Aluminum trioxide (Al <sub>2</sub> O <sub>3</sub> )	4.95	4.77
Iron oxide (Fe <sub>2</sub> O <sub>3</sub> )	3.66	3.39
Calcium oxide (CaO)	61.70	62.06
Magnesium oxide (MgO)	2.75	2.65
Sulfur trioxide (SO <sub>3</sub> )	2.16	3.26
Loss on ignition (LOI)	1.20	1.37

**Table 5.** Physical properties of the superplasticizer.

Main Component	Type	Density (g/cm <sup>3</sup> )	Usage (cement×%, mass ratio)
Polycarboxylic ether	Liquid	1.05	~ 0.8-1.2

product containing an anti-freeze agent was used as an accelerator, with characteristics shown in Table 6. The physical properties of the aggregates are shown in Table 7.

## Results and Discussion

### Flow characteristics

**Table 6.** Characteristics of accelerator for freeze protection.

Main Component	Type	Density (g/cm <sup>3</sup> )	Usage (cement×%, mass ratio)
Calcium formate	Liquid	2.15	~ 10-20

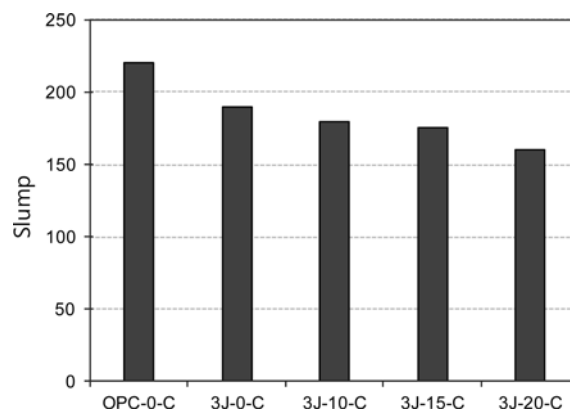
**Table 7.** Physical properties of aggregates.

Type	Density (t/m <sup>3</sup> )	Absorption (%)	Fineness modulus	Ratio of absolute volume (%)
Fine aggregate	2.60	1.45	2.16	63.72
Coarse aggregate	2.68	1.03	7.05	58.13

Fig. 3 shows the slump values of the concrete mixtures as a function of the replacement ratio of the accelerator. The experimental results show that the 3J-0-C specimen, which contains only HC, has a lower slump value than OPC-0-P, containing only OPC, and 3J-0-P, containing HC. This is caused by insufficient water absorption in 3J-0-C because of the increased Blaine fineness of HC. Moreover, the slump value decreased with the accelerator content for the samples containing HC. Both the water content and slump value decreased with the accelerator content.

### Setting times

Fig. 4 shows the setting times as a function of the concentration of the accelerator. The setting tests were performed at 20 °C, because solidification by freezing occurred similarly to solidification by hydration reactions at –5 °C. The results show that the setting times of OPC-0-C (plain OPC) and 3J-0-C, which contains only HC, are shorter than those of the other samples because of the differences between the intrinsic behaviors of the OPC and HC cements. Moreover, the setting time is decreased with increases in the accelerator content and for specimens containing HC. The final setting times of 3J-0-C and 3J-20-C,

**Fig. 3.** Slump test results.

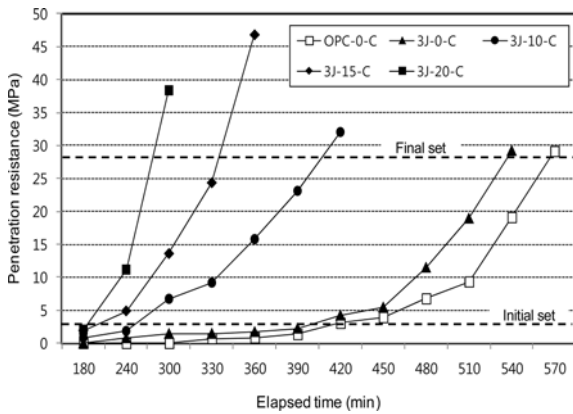


Fig. 4. Setting time test results.

with 0% and 20% accelerator, respectively, differ by 300 min. The setting time is shortened as the formation of the cement compounds  $C_3A$  and  $C_4AF$ , which affect cement solidification, is facilitated by the accelerator.

### Compressive strength

Fig. 5 shows the compressive strength data as a function of the accelerator content and aging time. Even though the compressive strength is increased with increases in the concentration of the accelerator, only the 3J-15-C and 3J-20-C specimens reach the required compressive strength of 5 MPa within one day of aging. However, OPC-0-C, containing only OPC, shows no increase in compressive strength. In addition, the samples containing the accelerator show higher compressive strengths throughout aging, with continuous strength development, compared to specimens without the accelerator. Thus, the addition of the accelerator does not affect the curing condition by temperature.

Comparing the results of the setting test with those from the quantitative analysis of  $Ca(OH)_2$  and the compressive strength experiments showed that increases in the concentration of the accelerator increased the compressive strength by reducing the setting time and accelerating  $Ca(OH)_2$  formation. Thus, it can be concluded that early frost damage could be prevented in wintertime concrete construction work without warm curing or heat curing by reducing the W/C ratio and optimizing the concentrations of high early strength cement and accelerator.

### $Ca(OH)_2$ formation

Fig. 6 shows the measurement results of  $Ca(OH)_2$  formation as a function of aging time.  $Ca(OH)_2$  formation is increased over the first day of aging with increases in the concentration of the accelerator. A comparison of  $Ca(OH)_2$  formation based on the cement type reveals that  $Ca(OH)_2$  formation in 3J-0-C, 3J-10-C, 3J-15-C, and 3J-20-C specimens containing HC is higher compared to that in OPC-0-C containing no HC. This result can be explained by the high Blaine fineness of HC and the differences between the two

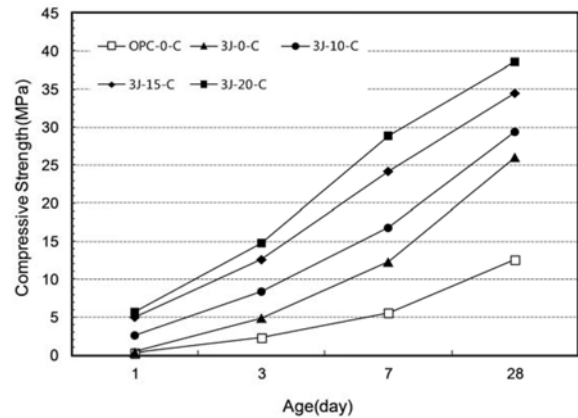


Fig. 5. Compressive strength test results.

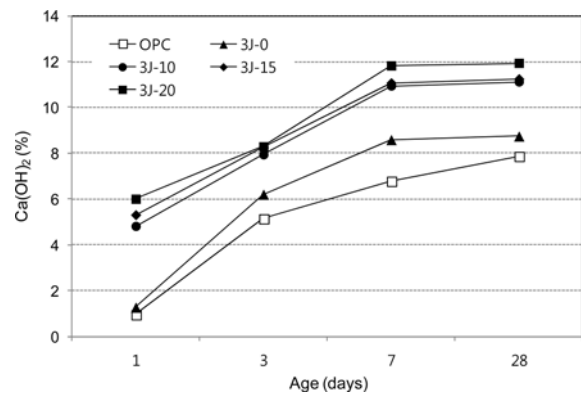


Fig. 6.  $Ca(OH)_2$  measurement results.

cement compositions. Moreover, an increase in the formation of  $Ca(OH)_2$  is observed with increases in the concentration of the accelerator. The  $Ca^{2+}$  ion, the main component of the accelerator, is dissolved, resulting in supersaturation in a short time. This affects the rate of  $Ca(OH)_2$  crystal reduction during  $Ca(OH)_2$  formation, wherein the  $Ca^{2+}$  ions in the cement are eluted in water and combined with the  $OH^-$  ions dissolved in water. In addition, by observing  $Ca(OH)_2$  formation over the 28-day aging period, the rate of  $Ca(OH)_2$  formation decreases after seven days. The increase in formation is decreased because  $Ca(OH)_2$  reacts with  $SiO_2$  in the cement over time, undergoing a phase change into C-S-H.

The addition of the accelerator promotes  $Ca(OH)_2$  formation early in the aging process. Since the rapidly generated  $Ca(OH)_2$  reacts with  $SiO_2$ , the rate of early age strength development is increased. Additionally, the strength is observed to develop quickly as the hydration products of C-S-H are formed early in aging.

### Conduction calorimetry

Fig. 7 shows the first peak in the hydration rate analysis using conduction calorimetry experiments as a function of the concentrations of OPC and accelerator. The results of the hydration rate experiments show that the early stage hydration heat is higher for specimens

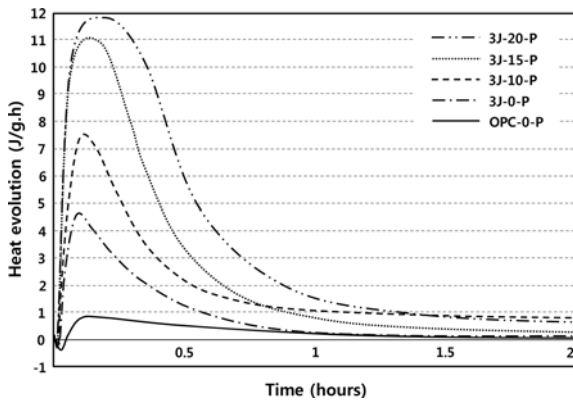


Fig. 7. Hydration heat of the first peak as a function of the concentration of accelerator.

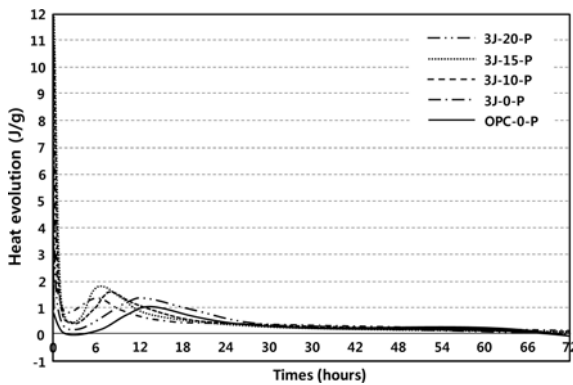


Fig. 8. Hydration heat of the second peak as a function of the concentration of accelerator.

containing HC compared to that of those using OPC. This originates from the high hydration heat, since water absorption is greater because of the increased Blaine fineness of HC compared to that of OPC. In addition, the hydration heat is increased with increases in the concentration of the accelerator. The accelerator is thought to stimulate the production of  $C_3A$  and  $C_4AF$ , the main hydration-heat cement products, thereby creating this first hydration peak.

Fig. 8 shows the second peak of the hydration heat curve over 72 hrs as a function of the concentration of the accelerator. These results show that the hydration rates of the specimens containing HC are higher than those of the specimens containing only OPC. In particular, the secondary peak related to the  $C_3S$  content appears in a short time with a high intensity. As the concentration of the accelerator is increased, the second peak is moved forward before the first peak vanishes, showing the increase in hydration rate. Acceleration in the  $C_3S$  hydration rate is observed with increases in the accelerator content. Thus, the addition of the accelerator enhances the hydration reaction of  $C_3S$  after 4 hrs, leading to greater strength development in the initial curing period, as observed from the hydration rate measurements.

**X-ray diffraction (XRD) results**

Figs 9(a-e) show the XRD diffraction patterns of the

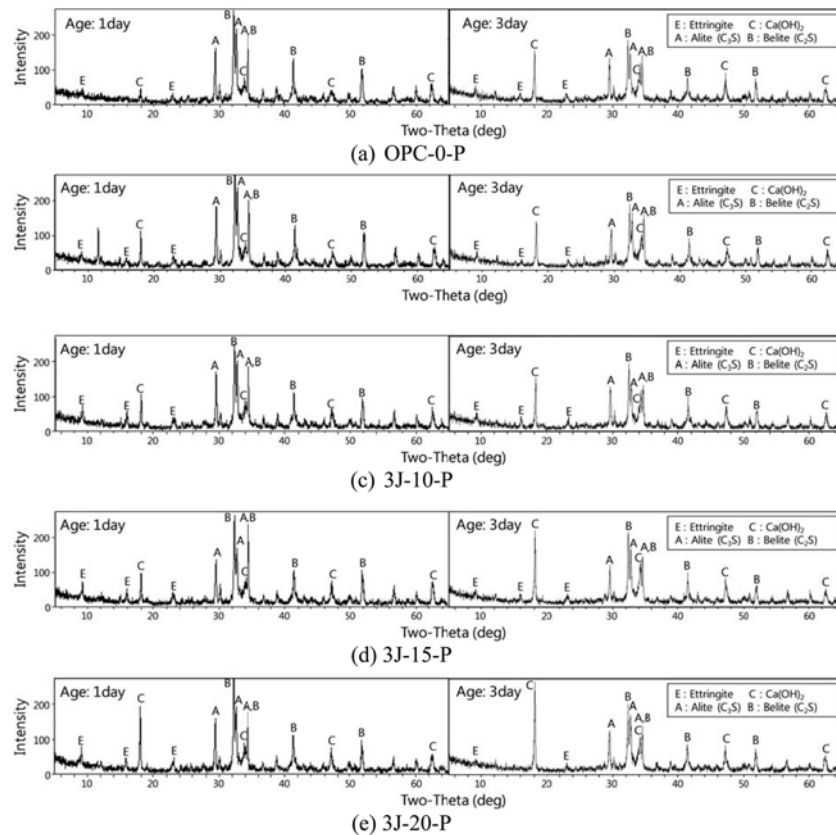


Fig. 9. XRD patterns of cement pastes after one and three days of aging.

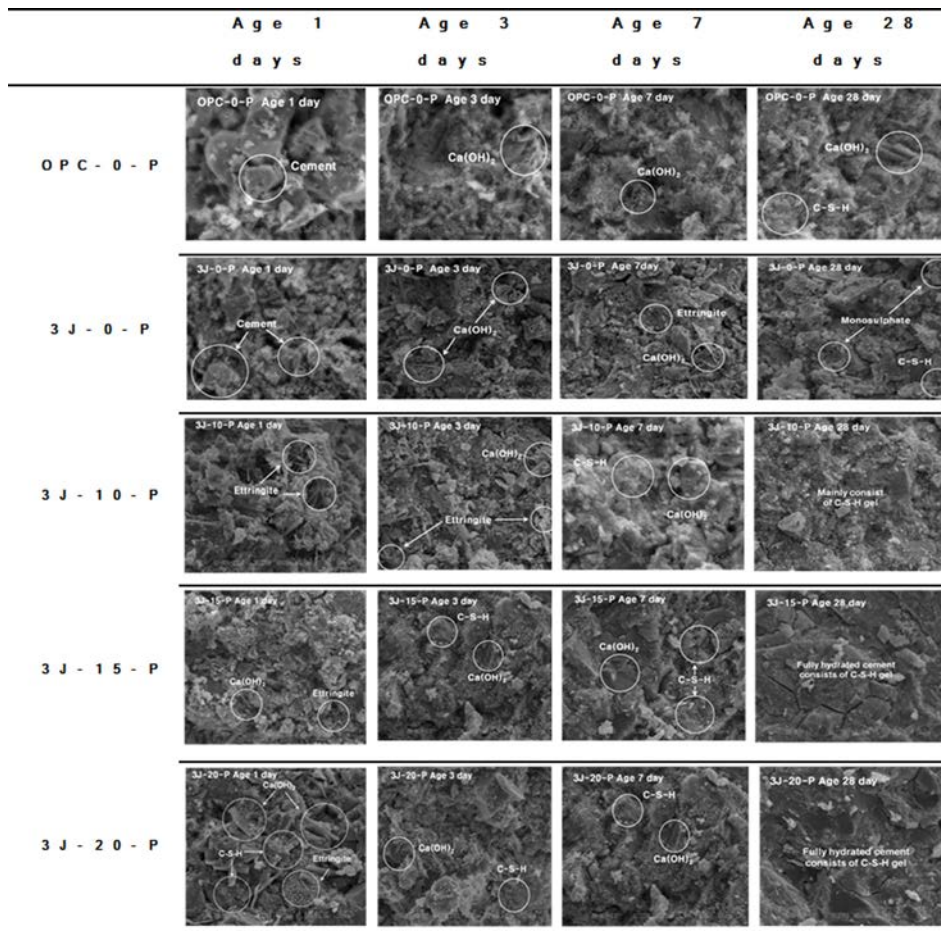


Fig. 10. SEM analysis results.

different cement pastes. In the case of OPC-0-P, weak ettringite and  $\text{Ca(OH)}_2$  peaks are observed after one day of aging. Meanwhile, high-intensity  $\text{C}_3\text{S}$  and  $\text{C}_2\text{S}$  peaks are found, showing that the majority of the cement is not hydrated, because water is unavailable in the frozen state at  $-5^\circ\text{C}$  without the presence of the accelerator for freeze protection. In addition, although many hydration products are generated in the 3J-0-P sample, which contains only HC, compared to OPC-0-P, the peaks related to the non-hydrated cement have high intensities. In Figs 9(c-e), showing the patterns of samples with both the accelerator and HC, the intensity of the ettringite and  $\text{Ca(OH)}_2$  peaks is increased with increases in the concentration of the accelerator. This is because the  $\text{Ca}^{2+}$  ions in the accelerator facilitate supersaturation concentrations in a short time, thereby affecting the rate of  $\text{Ca(OH)}_2$  crystal reduction. In addition, the peaks of ettringite and  $\text{Ca(OH)}_2$  hydration products are increased in intensity, while the  $\text{C}_3\text{S}$  and  $\text{C}_2\text{S}$  peaks are decreased in size with increases in aging time for all specimens. The intensity of the peaks from the cement compounds decreased, while that of those from the hydration products is increased because of the continuous hydration reaction between the cement and water. In summary, when the accelerator is present in the cement

mixture, the hydration reaction is enhanced since freezing of the sample is prevented at temperatures below  $0^\circ\text{C}$ .

### Microstructure

Fig. 10 shows the results of the SEM analyses at  $2000\times$  magnification, which are used to visually confirm the beginning of the formation of hydration products as a function of the concentration of the accelerator. These SEM images show that OPC-0-P, with neither HC nor accelerator, contains a large amount of non-hydrated cement after one day of aging, while fine hydration products are observed after three days of aging. In addition, after 28 days of aging,  $\text{Ca(OH)}_2$  and C-S-H hydration products are clearly observed. In the case of 3J-10-P, with 10% HC and accelerator, the ettringite hydration product is observed between cement particles after only one day of aging. These cement hydration products increase in quantity over time. The hydration reaction is significantly improved by the addition of the accelerator, compared to that observed in the OPC-0-P and 3J-0-P samples.

Moreover, cement hydration products are observed in the 3J-15-P and 3J-20-P specimens after one day of aging, while the C-S-H hydration product, which affects the strength, is observed within three days or

less of aging. In addition, the structure of the hydration products becomes finer over time. Thus, it can be concluded from the SEM analyses that the hydration reaction rate is increased with increases in the concentration of the accelerator, while the amount of hydration products is also increased. This finding is consistent with the results of the XRD analyses.

### Conclusions

1. The early-age compressive strength was increased and the setting time decreased with the concentration of the accelerator in the concrete. The accelerator prevented early frost damage to the specimens at temperatures below 0 °C and accelerated the cement hydration reaction.

2. The experimental results showed that a compressive strength exceeding 5 MPa, which was the objective of this research, could be obtained after one day of aging when 15% of accelerator was added.

3. The early-age compressive strength induced by the accelerator increased as  $\text{Ca}^{2+}$  ions, a major component of the accelerator, dissolved and facilitated rapid supersaturation. Meanwhile, the formation of  $\text{C}_3\text{S}$  was stimulated, which affected the reduction rate of  $\text{Ca}(\text{OH})_2$  crystals.

4. Because of the reaction of much of the  $\text{C}_3\text{S}$  in the accelerator and the high early strength cement, the rate of hydration heating and the amount of hydration heat increased. In particular, these acted to shift the second exothermic peak forward in time.

5. From the XRD analyses, we observed high-intensity ettringite and  $\text{Ca}(\text{OH})_2$  peaks early in the aging process because of the action of the accelerator, which showed that the hydration reaction was promoted. These results were consistent with the TG/DTA results and SEM analyses as functions of the aging times.

### Acknowledgments

This study is part of the output of the research funding for the Advanced-City Development Project 2015 of the Ministry of Land, Transport, and Maritime Affairs (15CTAP-C078650-01).

### References

1. R. Demirboğa, F. Karagöl, R. Polat, and M.A. Kaygusuz, *Constr. Build. Mater.* 64 (2014) 114-120.
2. F. Karagöl, R. Demirboğa, M.A. Kaygusuz, M.M. Yadollahi, and R. Polat, *Cold Reg. Sci. Technol.* 89 (2013) 30-35.
3. F. Karagöl, R. Demirboğa, and W.H. Khushefati, *Constr. Build. Mater.* 76 (2015) 388-395.
4. J.-S. Ryou and Y.-S. Lee, *Mater. Sci. Eng. A.* 532 (2012) 84-90.
5. K.-T. Koh, C.-J. Park, G.-S. Ryu, J.-J. Park, D.-G. Kim, and J.-H. Lee, *Nucl. Eng. Tech.* 45[3] (2013) 393-400.
6. S.-T. Yi, S.-W. Pae, and J.-K. Kim, *Constr. Build. Mater.* 25[3] (2011) 1489-1449.
7. C.K. Nmai, *Cem. Concr. Compos.* 20[2/3] (1998) 121-128.
8. ACI 306R-10, *Guide to Cold Weather Concreting*, American Concrete Institute, 2010.
9. ACI 306.1-90, *Standard Specification for Cold Weather Concreting*, American Concrete Institute, 2002.
10. L.V. Zinevich, *Mag. Civil Eng.* 2 (2011) 24-28.
11. L.A. Barna, P.M. Seman, and C.J. Korhonen, *J. Mater. Civ. Eng.* 23 (2011) 1544-1551.
12. A.F. Nassif and M.F. Petrou, *Constr. Build. Mater.* 44 (2013) 161-167.
13. M. Çullu and M. Arslan, *Compos. Pt. B-Eng.* 50 (2013) 202-209.
14. J.-S. Ryou and Y.-S. Lee, *Cold Reg. Sci. Tech.* 87 (2013) 1-5.
15. N.K. Ponomarev and B.G. Fomin, *Hydrotech. Constr.* 30[1] (1996) 39-44.
16. K.Y. Yuen, J.S. Ha, D.H. Lee, T.W. Park and J.Y. Won, *Archit. Inst. Korea. Struct.* 32 (2006) 55-62.
17. M.C. Han, *J. Korea. Inst. Build. Constr.* 16 (2016) 67-76.